Supplementary information II of ResMapper: A benchmark example of Istanbul, Turkey and parameter study

Byun, Ji-Eun

Engineering Risk Analysis Group, Technical University of Munich, Germany

Department of Civil, Environmental and Geomatic Engineering, University College London, UK

D'Ayala, Dina

Department of Civil, Environmental and Geomatic Engineering, University College London, UK

This supplementary document demonstrates the application of the ResMapper toolkit by investigating a benchmark example: Istanbul, Turkey consisting of 974 districts. Resilience loss values are evaluated for each district in terms of two types of network performance measure, i.e. the global efficiency and the connectivity to destination nodes. For the latter measure, three types of destination nodes are examined, i.e. motorways, hospitals and airports. Furthermore, to investigate impacts of the analysis parameters, additional analyses are performed with changed parameter values.

1. Data collection

The GIS data, i.e. roadways, vertices (the intersections of roadways) and districts, are downloaded from OpenStreetMap. Then, their join data are generated using ArcGis Pro 2.8.0. Also, to enable a large-scale analysis, the types of bridges and roadways are automatically classified based on the number of lanes and speed limits.

For seismic hazards, all districts are considered having the moment magnitude of 7.5, peak ground acceleration (PGA) 0.4 g and the spectral acceleration (Sa) at period 1 second as 0.5 g. Fragility curves, recovery curves and the proportion of soil vulnerability categories are adopted from FEMA (2020) [1]. On the other hand, the data of building damage is provided by Istanbul Metropolitan Municipality (IMM).

2. Results of benchmark analysis

Resilience loss values of districts are evaluated with regard to the global efficiency, which are mapped in Figures 1a and 1b respectively for the entire city and the central area. The map shows varying loss values across districts. To understand the distribution of the loss values of districts, a histogram is plotted in Figure 2. It is noted that the distribution has a long and heavy tail, which implies that some districts are subjected to particularly high consequences.

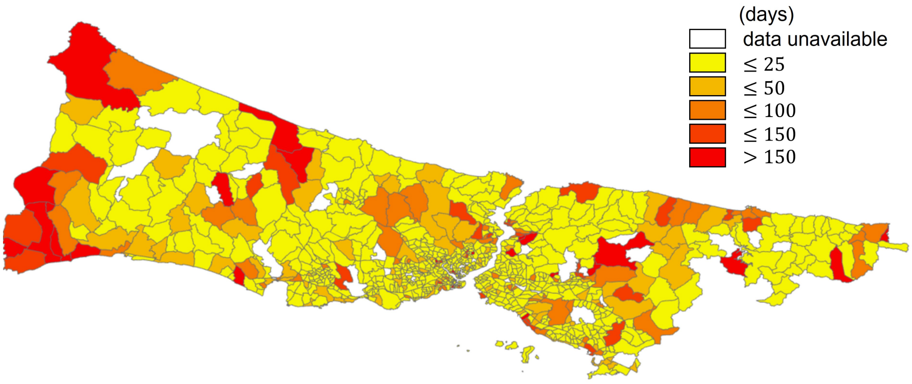

(a) Entire city

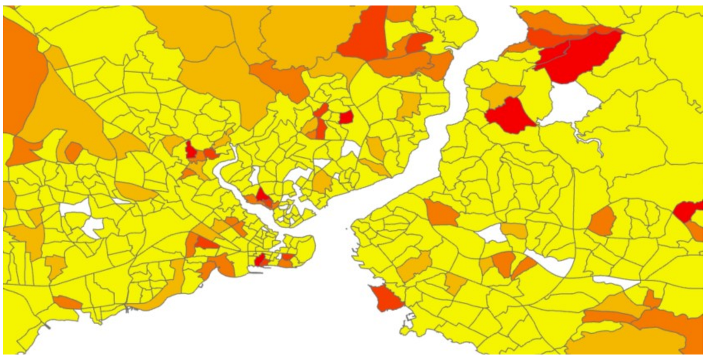

(b) Central area

Figure 1: Resilience loss map of global efficiency

Similar analyses are made in Figure 3 with respect to the connectivity to destination nodes. Figures 3a, 3b and 3c represent the resilience loss with respect to the destination nodes of airports, entrances to highways and hospitals, respectively. The comparison of the maps in Figures 1 and 3 suggests that there are correlations between the measures, while they still show some noticeable variations. In case of connectivity, outskirts districts

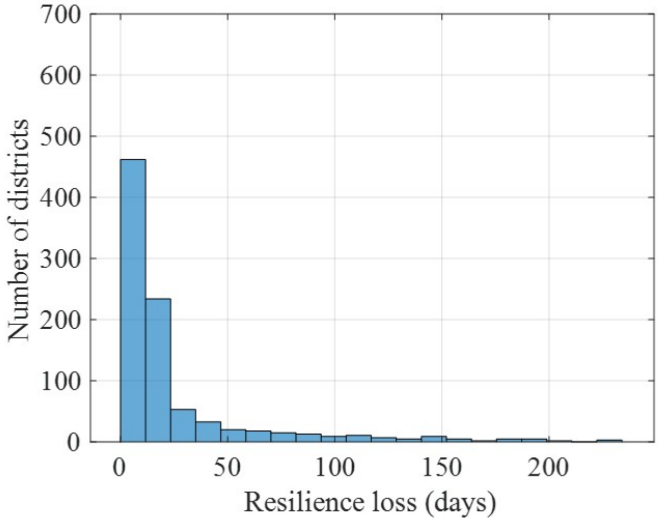

Figure 2: Histogram of resilience loss values of global efficiency

show high loss values as most destination nodes are concentrated in the central area.

Histograms of resilience losses in Figure 3 are also plotted in Figure 4. While the plots are similar to Figure 2, that of the connectivity to airports in Figure 4a has a different shape than others. This is owing to the fact that there are only a few airports.

3. Parameter study

The toolkit requires users to provide four types of parameters: the average length of buildings, the clearance resource units available per day (or another closely related parameter is the debris units generated by varying damage states of buildings), the ratio of road closure days to road recovery days, and the ratio of road closure days to the recovery days of overpasses. To understand the influence of these parameters, additional analyses are carried out with their values changed. This analysis can be understood either as an investigation of varying influences of parameters or as an investigation of decision scenarios deployable to moderate those parameters.

The average length of buildings is found to have a marginal influence compared to other parameters, leading to differences less than 3%. Therefore, the following discussions only illustrate the other three parameters.

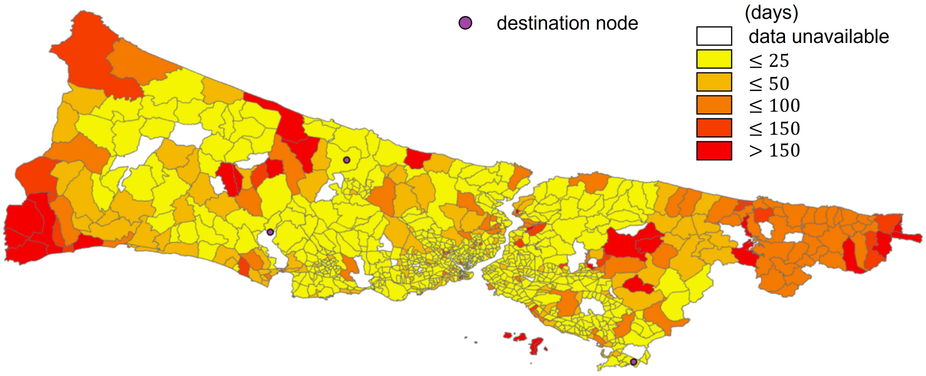

(a) Airports

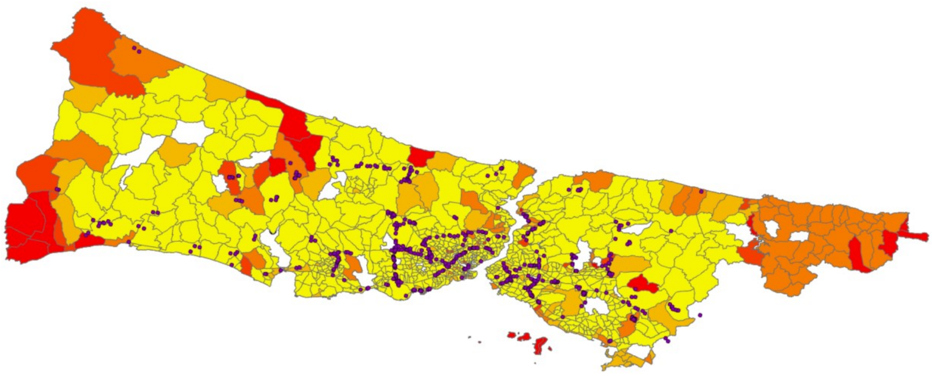

(b) Entrances to highways

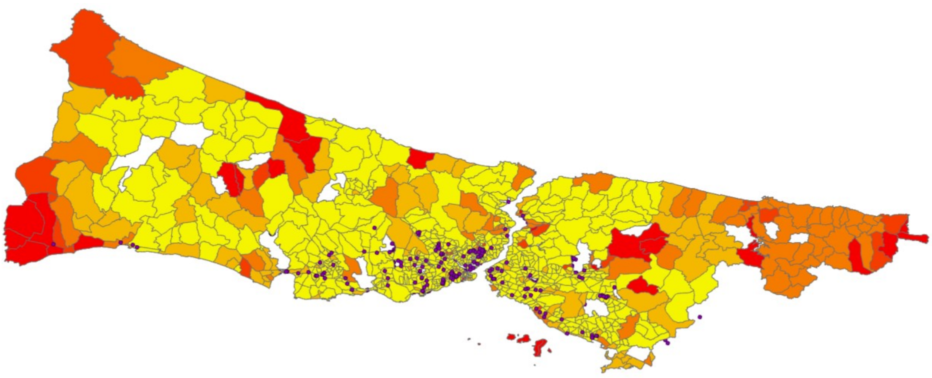

(c) Hospitals

Figure 3: Resilience loss map of connectivity to destination vertices

3.1. Change ratio in resilience loss

3.1.1. The amount debris cleared per day

To examine the effect of the process of the generation and clearance of building debris, the debris units that can be cleared a day are reduced to from

200 to 100. The difference in the resilience loss with respect to the global efficiency is mapped in Figures 5a and 5b, which respectively represent the entire city and the central area. The maps show that this parameter type has a great influence on the districts in the central area. This is as expected since the central area has a higher building density, whereby their resilience loss is greatly affected by building debris. The distribution of the differences is plotted in Figure 5c. The histogram suggests that the parameter has a great influence on the analysis result, incurring up to 50% difference.

3.1.2. Ratio of road closure days to road recovery days

The effect of the ratio of the closure days of a road to the number of its recovery days is investigated by increasing the parameter from 0.5 to 0.75. The difference in the resilience loss is mapped for the entire city and the central area respectively in Figures 6a and 6b. This parameter has great influences across districts, which is also confirmed by the histogram of the differences in Figure 6c.

3.1.3. Ratio of road closure days to the recovery days of overpasses

Another analysis is performed by changing the ratio of the closure days of a road to the recovery days of its overpasses, from 0.1 to 0.5. The change in the resilience loss values is mapped for the entire city and the central area respectively in Figures 7a and 7b. The two maps suggest that this parameter has irregular influences across districts. To examine the source of such variance, overpasses are illustrated in Figure 7b by green lines. It is found that the districts showing a high difference are where their major roads are laid under overpasses. For example, Figure 7c shows the map data of the area in the black box in Figure 7b. As indicated in the map, this sector consists of multiple major highways, i.e. O-1, O-4 and D100, which are overlapped to each other. Accordingly, the resilience loss of this district is highly sensitive to this parameter. Such wild variation is also confirmed by the histogram of the difference in Figure 7d. In the histogram, while most districts show low differences, the distribution of the differences has a very long tail.

3.2. Change in the order of resilience loss

In contrast to Section 3.1, this section investigates if the parameters change the relative order of the resilience loss values between districts. Such analysis is relevant to decision tasks of allocating limited resources to districts, in which case analysis interests would lie in the relative values of districts rather than absolute values.

Figures 8 and 9 show the maps of the global efficiency, respectively over the entire city and the central area. By comparing the maps with that of reference parameters in Figure 1, two observations are drawn. First, the relative order between districts is relatively insensitive to the change in the parameters, i.e. the districts with higher loss values remain higher than other districts. This suggests that the analysis is robust for the purpose of ordering the districts. Therefore, in this case, the parameters do not need to be fine-tuned. Second, districts show varying sensitivity to the parameters. Some districts show particularly high sensitivity to certain parameters, which sometimes reverse their relative order. Such districts need an extra attention as a higher sensitivity implies a higher likelihood of high-consequence events and a greater effectiveness of relative measures.

4. Concluding remarks

This supplementary document illustrates the implementation of ResMapper. To this end, a benchmark network of Istanbul in Turkey is examined. The example demonstrates the applicability of the toolkit for large-scale networks as the city involves 974 districts. The evaluated maps show the varying resilience from district to district. The results indicate that such resilience is determined by the interplay of various factors (e.g. hazard risks, network topology and fragility of roads and buildings) as well as by a chosen network performance measure (i.e. the purpose of a network).

The parameter study reveals that there are three critical parameters: the debris generation/clearance process of buildings, the ratio of the closure days of a road to its recovery days and that with regard to its overpasses. The results show that the parameters have critical influences on analysis results. Moreover, the parameters have varying influences on districts depending on the characteristics of the districts. This implies that different districts require different decisions for an effective management of resilience. On the other hand, it is found that the parameters do not have significant impacts on the relative order of resilience loss between districts. Such results indicate that while the parameters play an critical role in determining the absolute values of resilience loss, they do not need to be fine-tuned if an analysis purpose lies in ordering the resilience of districts (e.g. allocating resources or identifying the most effective measures for each district).

References

[1] FEMA, Hazus earthquake model technical manual (2020).

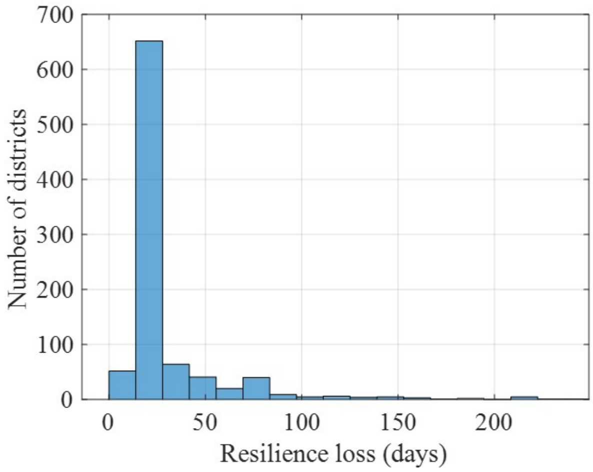

(a) Airports

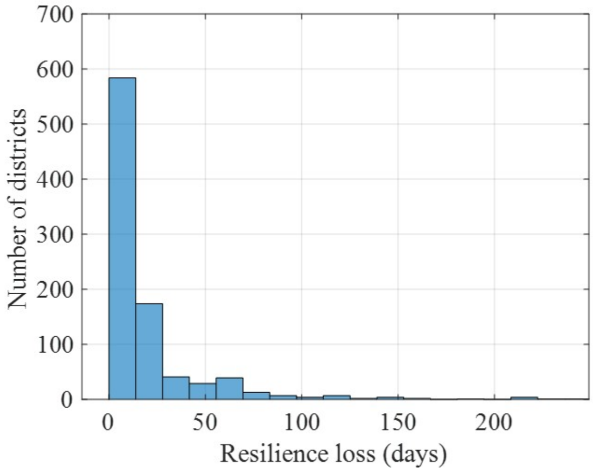

(b) Entrances to highways

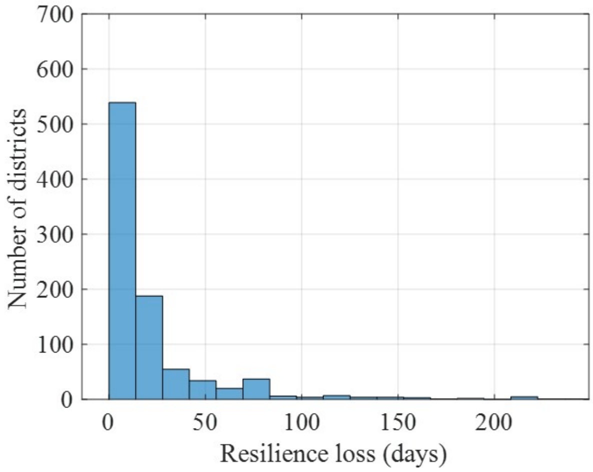

(c) Hospitals

Figure 4: Histogram of resilience loss values of connectivity

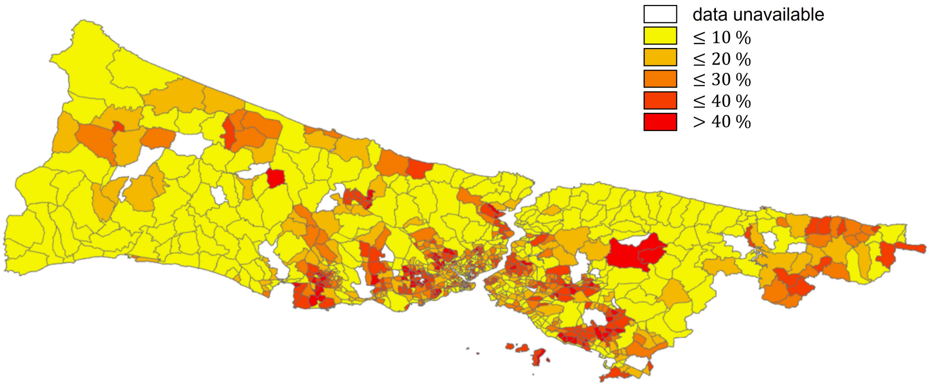

(a) Entire city

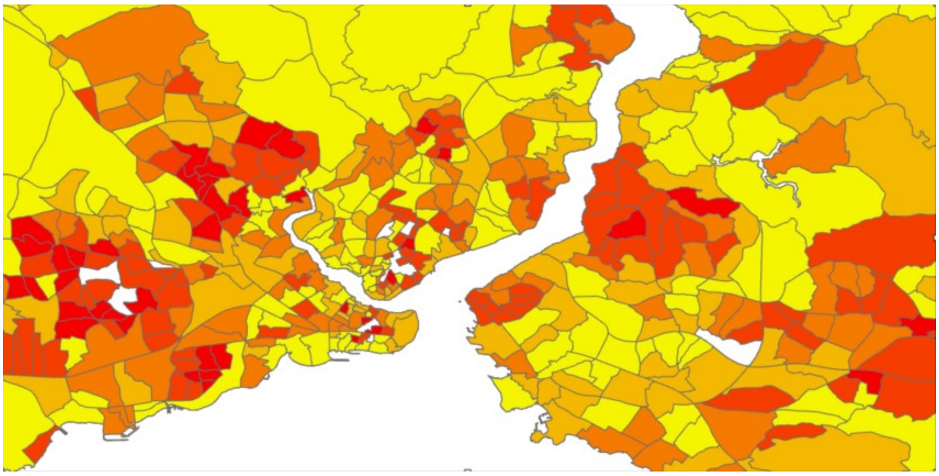

(b) Central area

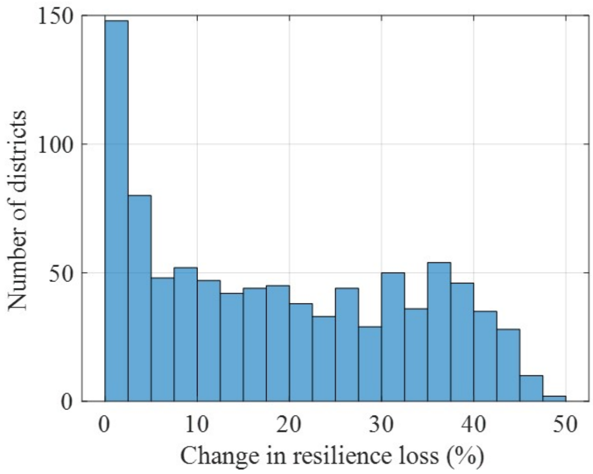

(c) Histogram

Figure 5: Change in resilience loss values with respect to the global efficiency by change in parameters related to building debris

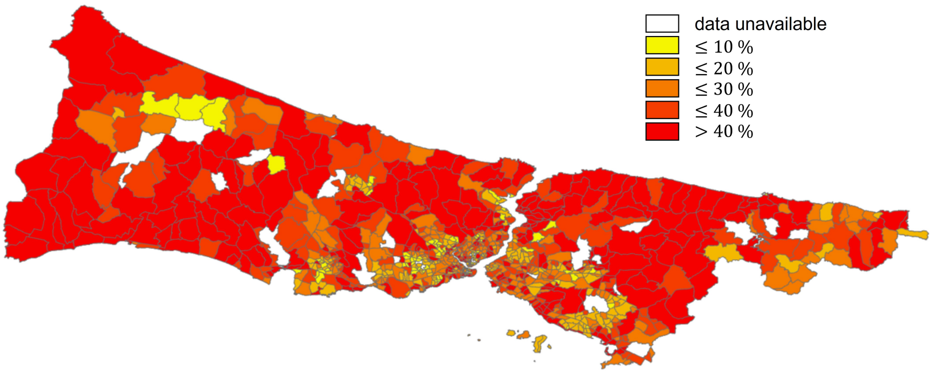

(a) Entire city

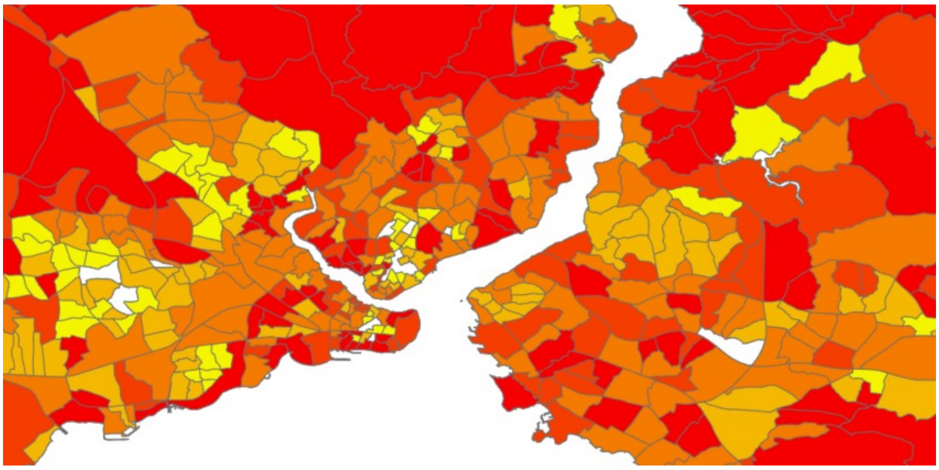

(b) Central area

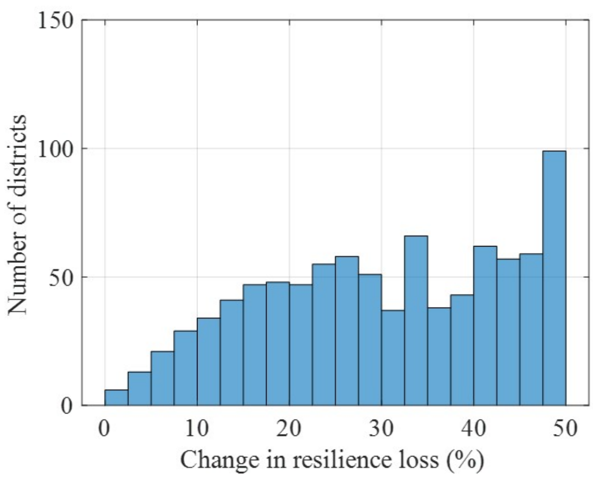

(c) Histogram

Figure 6: Change in resilience loss values with respect to the global efficiency by change in the parameter of the ratio of road closure days to road recovery days

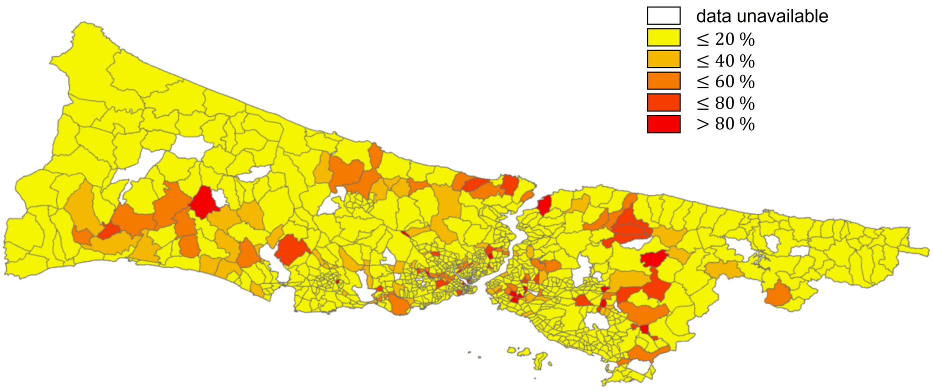

(a) Entire city

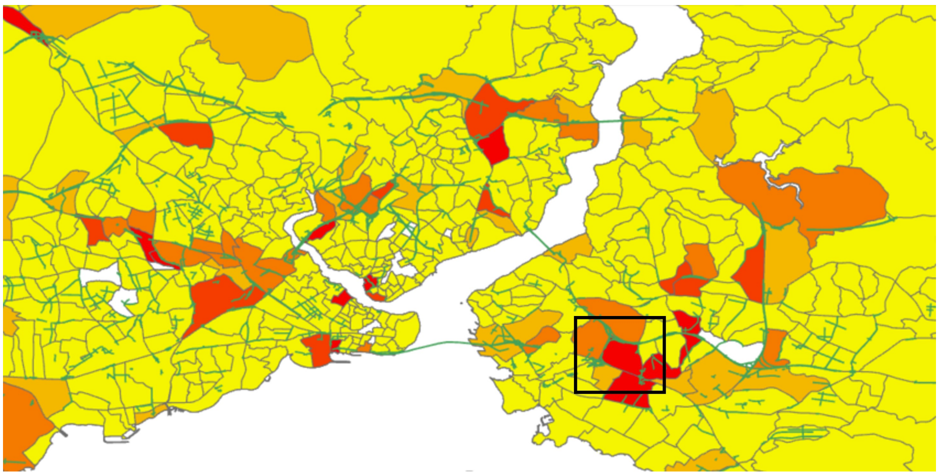

(b) Central area

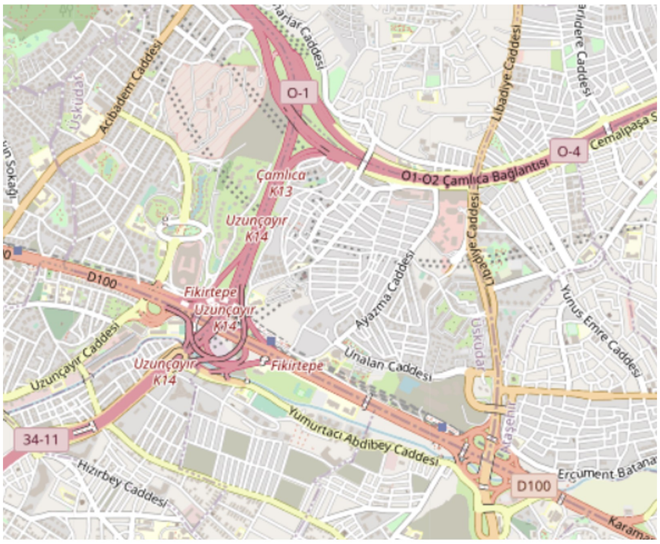

Map Image from © OpenStreetMap

(c) Map data of the black box in Figure 7b

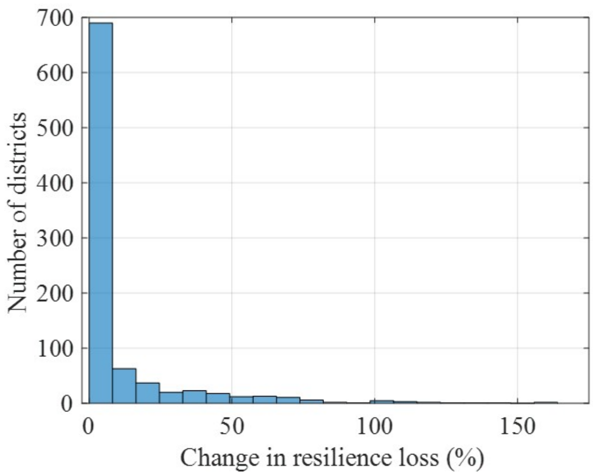

(d) Histogram

Figure 7: Change in resilience loss values with respect to the global efficiency by change in the parameter of the ratio of road closure days to recovery days of overpasses

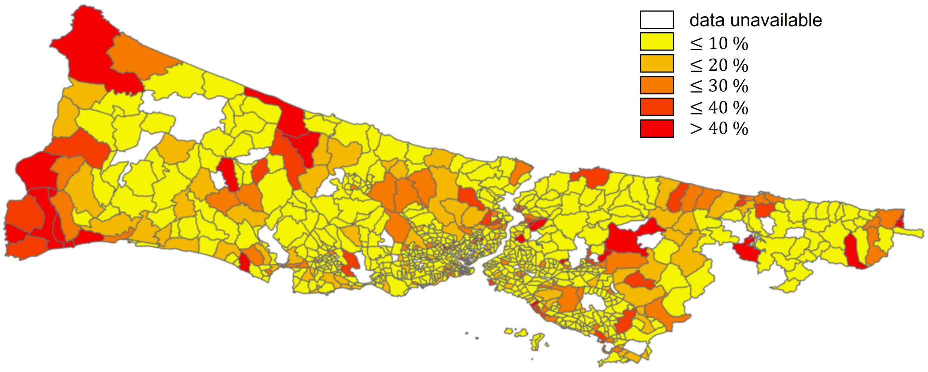

(a) Parameter of building debris clearance

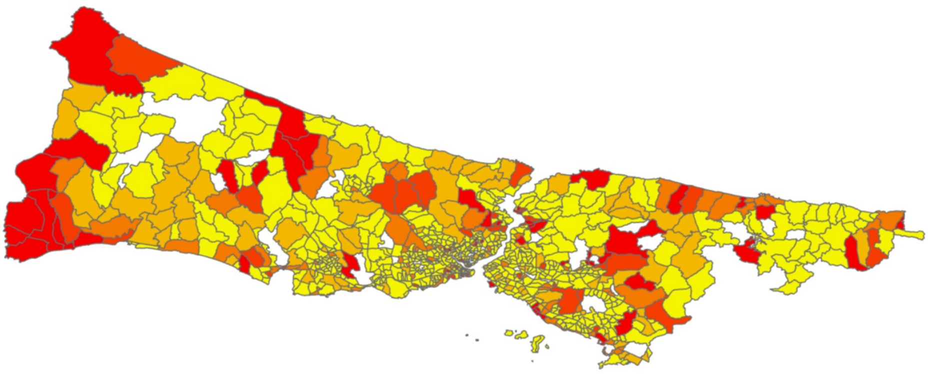

(b) Ratio of road closure days to road recovery days

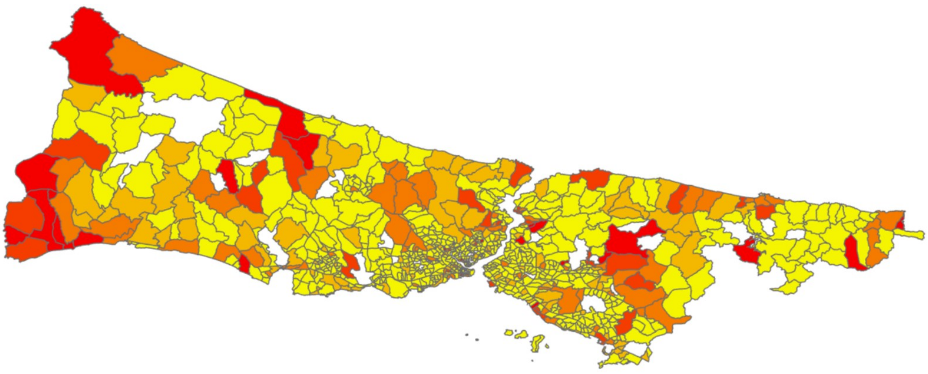

(c) Ratio of road closure days to recovery days of overpasses

Figure 8: Resilience loss map of global efficiency with changed parameters

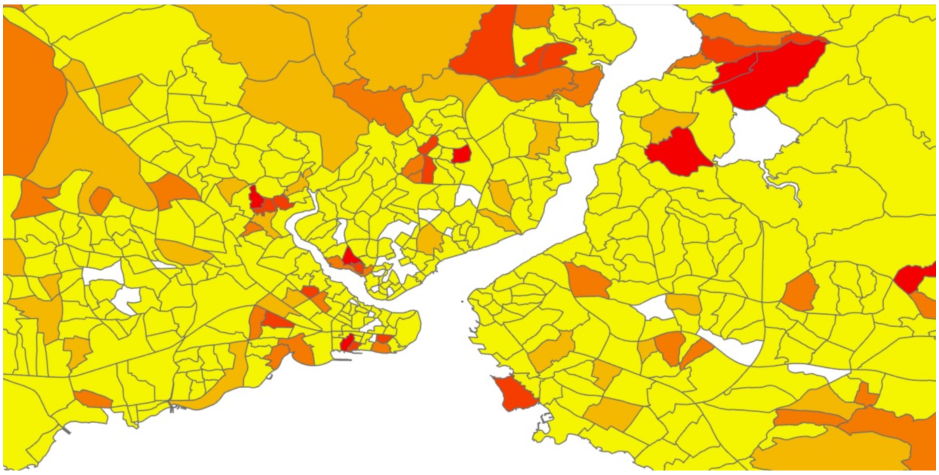

(a) Parameter of building debris clearance

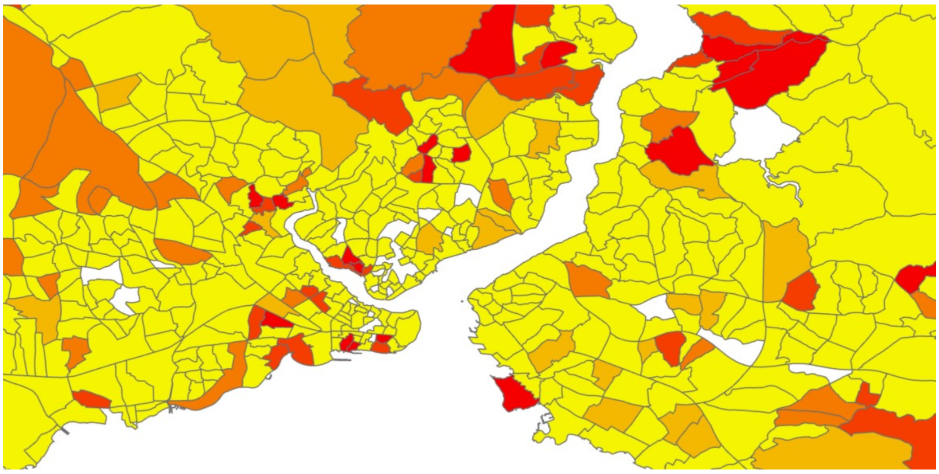

(b) Ratio of road closure days to road recovery days

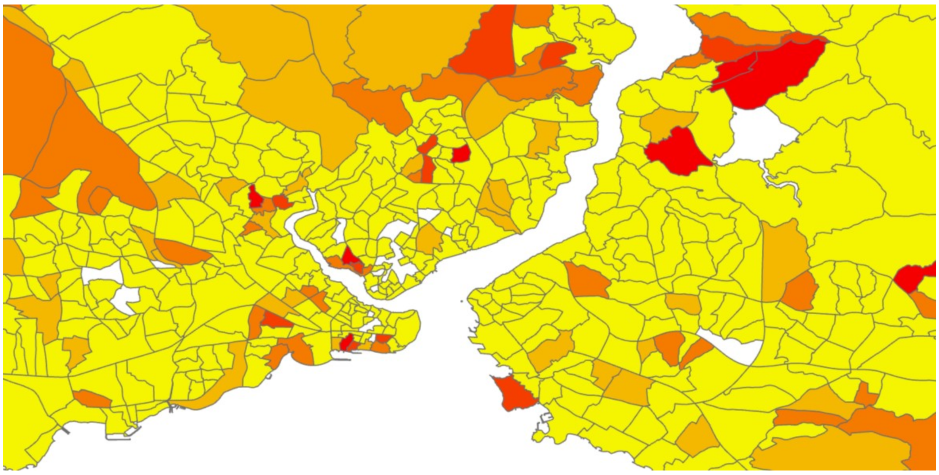

(c) Ratio of road closure days to recovery days of overpasses

Figure 9: Resilience loss map of global efficiency with changed parameters – Central area